

## MARS POLAR LANDER APPROACH NAVIGATION

**P. D. Burkhart, V. Alwar, S. W. Demcak\*, P. B. Esposito, E. J. Graat,  
V. M. Pollmeier, B. M. Portock, M. S. Ryne**

Jet Propulsion Laboratory  
California Institute of Technology  
Pasadena, California 91109  
Email: Dan.Burkhart@jpl.nasa.gov

Mars Polar lander, launched on January 3, 1999, arrived at Mars on December 3, 1999. This paper concentrates on the navigation analysis required to meet the arrival criteria necessary to land at the desired landing site (195° west longitude and 76° south latitude) and simultaneously deliver two microprobes to Mars entry conditions. Results are presented for approach navigation using near-simultaneous tracking data collected from both Mars Polar Lander and Mars Global Surveyor and using tracking data from Mars Polar Lander only.

### INTRODUCTION

On January 3, 1999, the Mars Exploration Program continued its exploration of the red planet with the launch of Mars Polar Lander, following the launch of the Mars Climate Orbiter on December 11, 1998. The objective of the Mars Polar Lander mission was a soft landing on the south polar layered terrain of Mars on December 3, 1999, followed by a three-month science mission. The science payload included an integrated suite of geochemistry and meteorology instruments called the Mars Volatiles and Climate Surveyor (MVACS), as well as the Mars Descent Imager (MARDI), and a Lidar instrument supplied by the Russian Institute for Space Science. In addition, two experimental microprobes were carried to Mars attached to the cruise stage.

After launch, problems with the star cameras were encountered. The spacecraft orientation limits for valid operation were found to be tighter than pre-launch testing indicated. The planned spacecraft attitude profile no longer was in the valid region for star camera operation, so a new attitude profile was required. Work on this profile continued through the increased tracking period the first 30 days of flight for several months. This redesign also forced additional analysis of spacecraft models, including the attitude control system modeling and the spacecraft component model used for solar radiation pressure acceleration calculation. Additional analysis was performed throughout cruise to assess the impact of the new attitude profile on the delivery accuracy.

---

\* OAO Corporation, Altadena, CA

The majority of spacecraft functions were performed by the lander, contained during cruise within an aeroshell. Communication with the Deep Space Network (DSN) was performed via the medium gain antenna (MGS), but was limited to four hours of continuous operation before a five-hour off time was required. Attitude control for the three-axis stabilized spacecraft was performed using a thruster-based attitude control system. Since the attitude control thrusters were uncoupled, telemetry data for the thruster activity was transmitted to the navigation team for use in the orbit determination process. The data for the many thousands of thruster pulses required careful monitoring, along with significant effort for calibration and validation. The attitude control activity was the major driver in the achievable delivery accuracy, in addition to maneuver execution error. Four trajectory correction maneuvers (TCMs) were planned, along with two contingency maneuvers to allow for a change in the landing site and to allow for a TCM 6.5 hours before entry<sup>3</sup>. The maneuvers executed through TCM4, along with the execution dates, are shown in Figure 1.

After the loss of Mars Climate Orbiter in late September, a navigation advisory Group (NAG) was formed. The initial purpose was an independent review of the MPL navigation plan and orbit determination (OD) results in detail, with the power to recommend modification of the plan and to assist in analysis of the required models to improve the fidelity of the navigation system. Filter and modeling improvements were formulated and refined by the NAG, then passed on to the navigation team for implementation in the operational navigation delivery process. This reduced the required workload of the navigation team by narrowing the list of solution strategies to implement. A brief safe mode entry on October 11 was the only other anomaly to impact the cruise

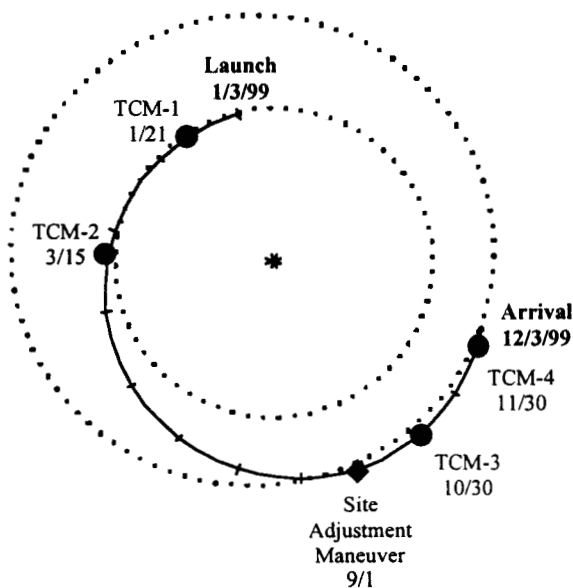


**Figure 1 Mars Polar Lander Transfer Trajectory**

trajectory, introducing additional perturbations to the flight path. Single four-hour tracking passes were executed daily after the first 30 days to 45 days before Mars encounter (E-45), when three four-hour passes per day were planned for the remainder of cruise. In addition, near simultaneous tracking (NST) data was collected using Mars Global Surveyor (MGS) as a navigation aid for more accurate Mars-relative navigation. NST data was collected until the TCM4 execution at E-3 days. Continuous tracking was scheduled for the remaining days of cruise before Mars encounter and the start of the Entry, Descent and Landing (EDL) phase.

Contact was lost as expected shortly before atmospheric entry, but was never regained. The EDL events were planned to unfold as follows. Five minutes before entry, the cruise stage was jettisoned, which included four solar panels, redundant star cameras and sun sensors, the Deep Space 2 microprobes and low- and medium-gain radio antennas (See Figure 2). The microprobes were deployed automatically approximately ten seconds after the lander separated from the cruise stage. Following hypersonic entry of the lander, the heatshield was jettisoned and a parachute was deployed. Finally, the lander was released from the backshell. The lander then performed a powered descent to a soft landing using radar-aided inertial guidance to a target site of 195° west longitude and 76° south latitude.

Landing at the south pole of Mars posed a challenging navigation problem. For polar entry, the flight path angle is dominated by errors normal to the orbit plane, the most difficult component to determine. For equatorial entry, the flight path angle is in the orbit

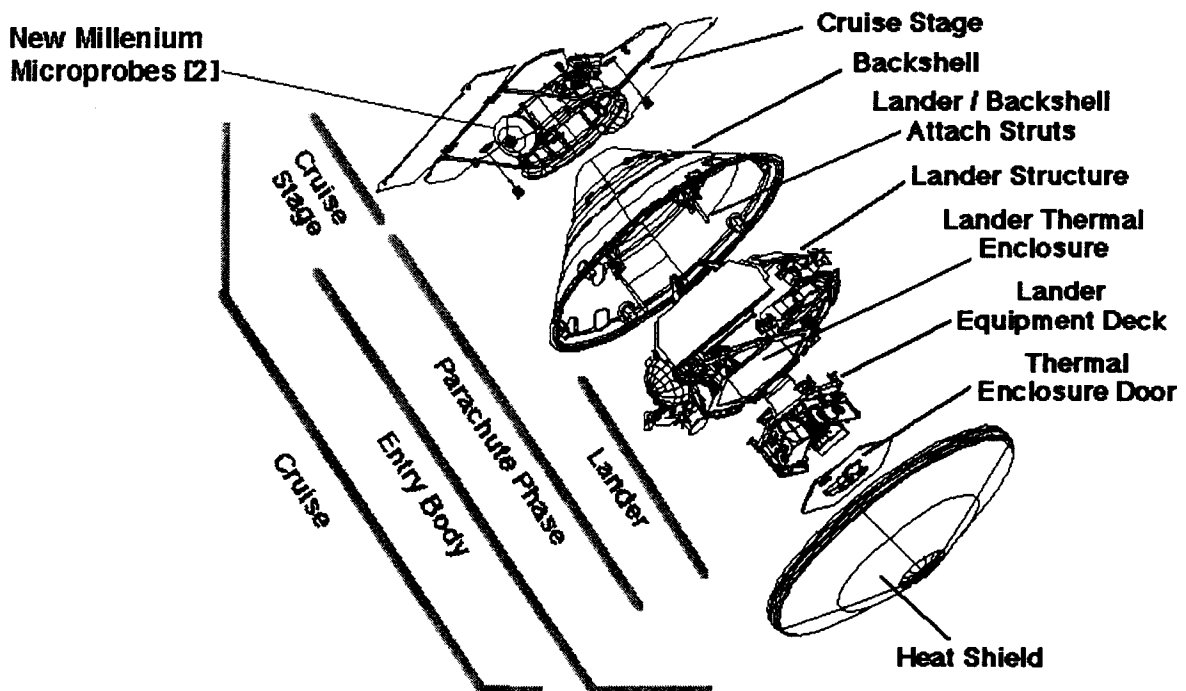


**Figure 2 Mars Polar Lander Flight System**

plane and less difficult to determine. The attitude control thruster activity was recognized before launch as a major error contributor, but this was further complicated by the additional attitude changes required for star camera processing. The use of NST was expected to reduce these errors, but the data type was relatively untested in flight.

This paper deals with the navigation analysis required to meet the landing site accuracy requirements. The spacecraft models developed before launch and after the star camera anomaly are discussed in detail, along with the tracking data strategy and the filter setup. Approach navigation results for both MPL only and combined MPL and Mars Global Surveyor (MGS) filter processing are presented.

## **SPACECRAFT MODEL**

The spacecraft modeling problem for MPL involved coping with a three-axis stabilized spacecraft with a thruster-based attitude control system, as opposed to momentum wheel control for most orbiters and spin stabilization used for Mars Pathfinder. This modeling was complicated by required changes in the attitude profile after launch due to star camera processing problems, as was the spacecraft component model used for solar radiation pressure acceleration calculation. These models are covered in detail below.

### **Attitude Model**

The pre-launch attitude model had the medium gain antenna (MGA) pointed at the Earth during tracking passes and the solar array pointed at the Sun during out-of-contact periods, with the spacecraft X-Z plane in the Sun-probe-Earth plane. The definitions used for Sun- and Earth-point determination are shown in Figure 3. This resulted in an attitude profile that changed daily early in cruise, but remained nearly constant (by design) during the last 60 days of cruise. The attitude deadband profile used with the above attitude definitions had smaller tolerances for tracking passes than during out-of-contact periods, along with different values based on mission day.

After launch, it was quickly determined that the star cameras could not operate with the array oriented at the Sun or with the medium gain antenna (MGA) pointed at the Earth, requiring modification to the original attitude profile. Since the star cameras are required to update the onboard attitude knowledge, the attitude profile during non-contact periods was modified to orient the star camera for proper operation. For communication periods, star camera processing was disabled.

From mid-January until early March, the spacecraft maintained a constant attitude that met all requirements for power, thermal, communication and star camera processing. The profile had the X-Z plane in the Sun-probe-Earth plane, with the MGA rotated  $27^\circ$  away from the Earth. The deadband profile was also modified to be  $\pm 9^\circ$  for X,  $\pm 6^\circ$  for

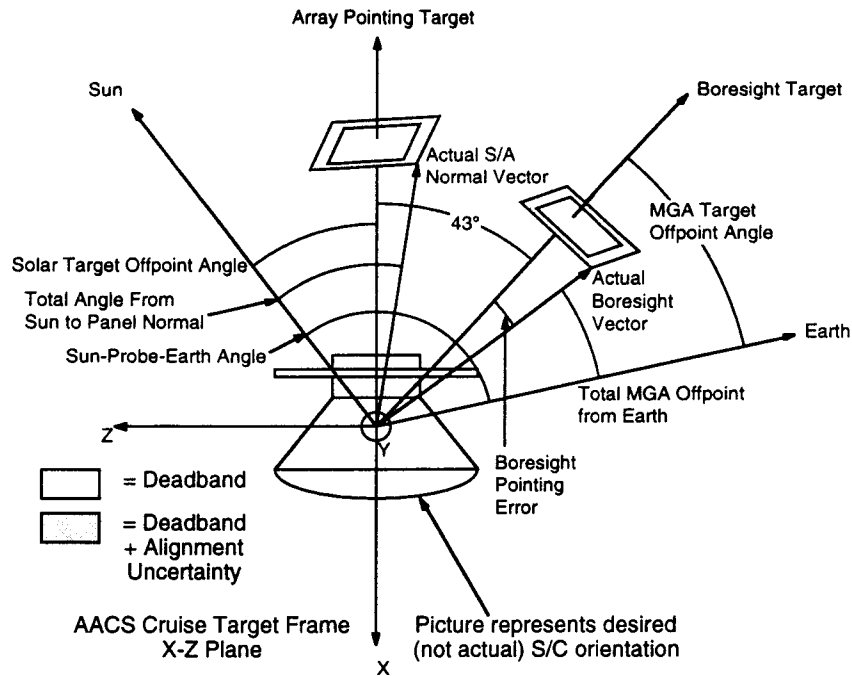


**Figure 3 Cruise Attitude Definitions**

Y and  $\pm 3.9^\circ$  for Z. These values were smaller than the original non-comm deadbands, but were larger than the original comm deadbands. These deadbands were used for the remainder of cruise.

In March, the attitude profile was modified since the requirements for power, communication and star camera processing could not be met with a single attitude profile. The resulting profile included an attitude for star camera operation that also satisfied the power and thermal requirements (star camera attitude) and an attitude for MGA contact with the Earth (comm attitude). The star camera attitude had the  $-X$  axis rotated  $25^\circ$  from the Sun in the Earth direction, plus a rotation of the X-Z plane out of the Sun-probe-Earth plane via rotation about the  $-X$  axis by  $20^\circ$ . The planned comm attitude was the same as the original comm attitude, with the MGA pointed directly at the Earth. This strategy was maintained for the remainder of cruise. From early March until October 11, the spacecraft maintained the star camera attitude except during scheduled tracking passes. For the last 45 days of cruise, with three scheduled tracking passes per day, this plan would have executed six attitude changes per day. This would have substantially increased the induced velocity on the spacecraft. In an effort to reduce the number of attitude changes as much as possible and thus the thruster activity, a new strategy was designed to remain at the comm attitude as long as possible between star camera updates. The minimum star camera processing required was one four-hour processing period every two days, but a test period was planned with one four-hour star camera period every day. So, from October 11 to November 4, the star camera attitude was used for four hours per day, with the remaining time spent at the comm attitude. From November

4 to the end of cruise, the star camera orientation was reduced to four hours every other day.

The most significant impact of the star camera problems in terms of attitude was larger differences between the star camera attitude and comm attitude during the last 60 days of cruise. The assumption of a nearly constant attitude during the last 60 days of cruise was no longer valid. For navigation software implementation and modeling accuracy reasons, the new attitude profile required the use of a file-based attitude model that was not necessary with the original profile. The original implementation approach was limited to 200 attitude changes, which was not enough inputs to accurately model the profile. With the unlimited inputs available using file-based approach, all of the attitude segments could be modeled.

In order to generate the most accurate model possible, attitude data from the small forces telemetry were used. The telemetry includes data for each attitude maintenance event, along with the spacecraft attitude quaternion at the time of the thruster firing. By definition, these reported attitudes have at least one axis at the deadband limit. So, for the profile, the average attitude was computed over intervals between orientation changes. It was possible to determine from the thruster firing history the start and end times of the deadband walks, so the intervals of constant commanded attitude could be determined. With this data an average attitude over the comm and star camera attitudes was computed, along with deadband walk durations for modeling the change from one attitude to the other. This process required some manual editing but was largely automatic. A plot showing the raw attitude data and the resulting attitude model for the last seven days of cruise are shown in Figure 4. The change in sign on DOY 334 was due to the approach used to slew to and from each maneuver attitude (in this case, TCM4). This involved rotating the spacecraft through a complete 360° in rotating to and from the maneuver attitude to minimize the resultant velocity perturbation. The majority of the shown profile represents the comm attitude, with short periods every other day at the star camera attitude.

### **Attitude Control Model**

Mars Polar Lander was three-axis stabilized during cruise, unlike the spin-stabilized Mars Pathfinder. Attitude maintenance and maneuvers were performed using a suite of eight monopropellant thrusters. The four maneuver thrusters were oriented normal to the solar arrays, while the attitude control thrusters were canted as shown in Figure 5 and oriented such that all combinations of thrusting used for attitude maintenance would have a resultant velocity change opposite the solar array normal.

Due to the tight entry corridor requirements, the baseline plan included telemetry replay of all attitude control thruster firings. During nominal cruise, telemetry for each thruster firing, including time, accumulated on time for each thruster, velocity imparted and the spacecraft attitude, was reported. The expected rate of thruster firings during nominal cruise was one event every 20 to 30 minutes. Since the firings were used to impart

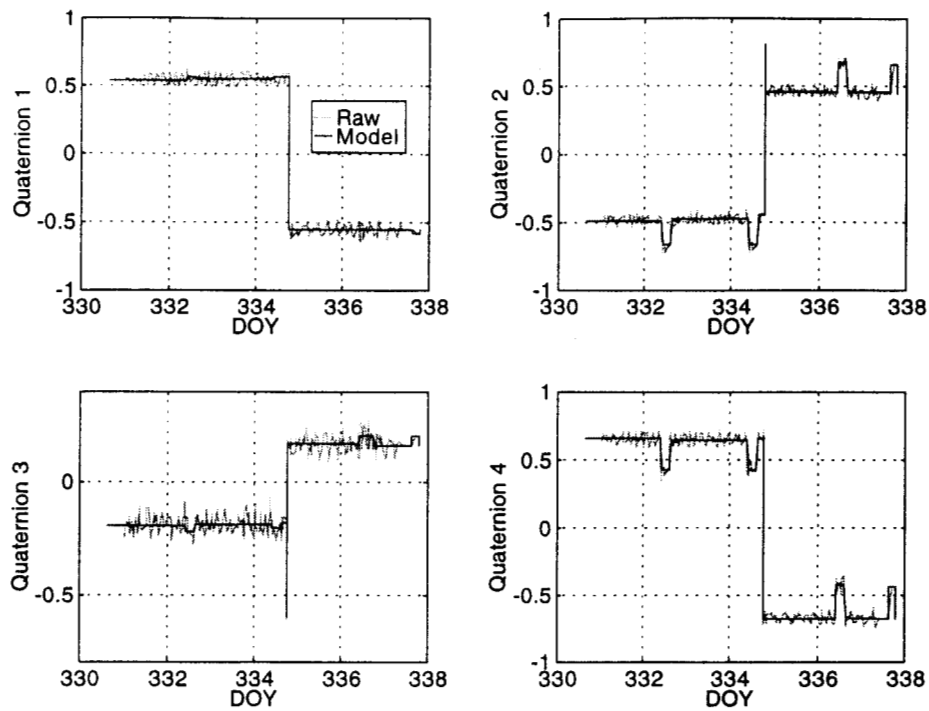


**Figure 4 File-Based Attitude Model and Raw Quaternions**

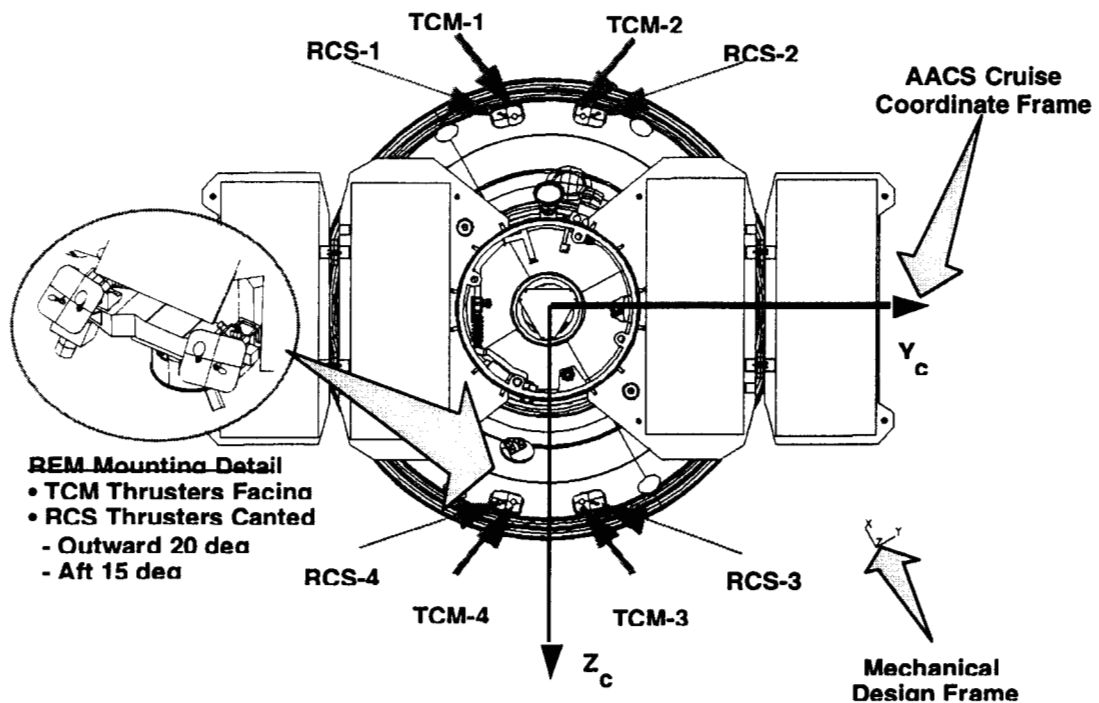


**Figure 5 Thruster Geometry**

rotations on the spacecraft, the thruster firings were nearly always in pairs. The exceptions to this telemetry reporting were for safe mode events (telemetry data included accumulated firings over 10 minute periods with average attitude reported) and during spacecraft slews to and from maneuver attitude (telemetry reported 15 second accumulated firings). In order to minimize the impact of slew activity on the desired velocity change for each maneuver, the combination of the slew to and the slew from the maneuver attitude would result in a 360° rotation of the spacecraft and cancellation of a significant portion of the slew velocity imparted.

A prediction model was developed before launch for trajectory propagation from the end of reconstructed thruster activity to Mars encounter. This model was based on the deadband profile, propellant tank pressure and spacecraft mass. Provisions were made in the development of this predictor for modifications to the predicted velocity change based on calibration with the reconstructed data.

The attitude profile changes in early March caused by the star camera problems not only increased the complexity of the attitude model but also increased the attitude control thruster activity. Additional thruster activity was introduced by the tighter deadbands used for the star camera attitude, but these were partially offset by the looser comm deadbands. The majority of this increase was due to the addition of deadband walks required to change the orientation from the star camera attitude to the comm attitude and back. This is illustrated in Figure 6 for the last week of cruise, which shows accumulated velocity in each of the spacecraft coordinate axes. The X velocity from each pulse is positive due to the thruster alignment discussed before, while the resultant velocity in the Y and Z axes are both positive and negative. The slew activity to orient for TCM4 is clearly visible in the Y and Z directions late on DOY 334. The additional thrusting for the deadband walks to and from the star camera attitude are visible in the X axis plot as increased slope on the even days. The deadband walk activity largely cancels in the Y and Z axes, with jumps that show several pulses in one direction followed by several in the opposite direction for the start and stop of the deadband walk. The deadband walk activity in the X axis is nearly 50% of the total thruster activity while the Y and Z axis contributions to the total imparted velocity are smaller due to cancellation. However, this additional activity in the Y and Z axes is significantly higher than during constant attitude periods, which will affect the error assumptions used in the filter.

The modifications in the attitude profile in October (one four-hour star camera period each day) was essentially the same as far as imparted velocity, effectively a change in which attitude was maintained longer. However, with star camera processing periods scheduled every other day in November, the number of deadband walks was cut in half, reducing the total imparted velocity.

The velocity imparted on the spacecraft due to attitude control was scrutinized from launch both for reconstruction and prediction calibration, but the most progress occurred during the increased tracking intervals the first 30 days and the final 45 days of cruise.



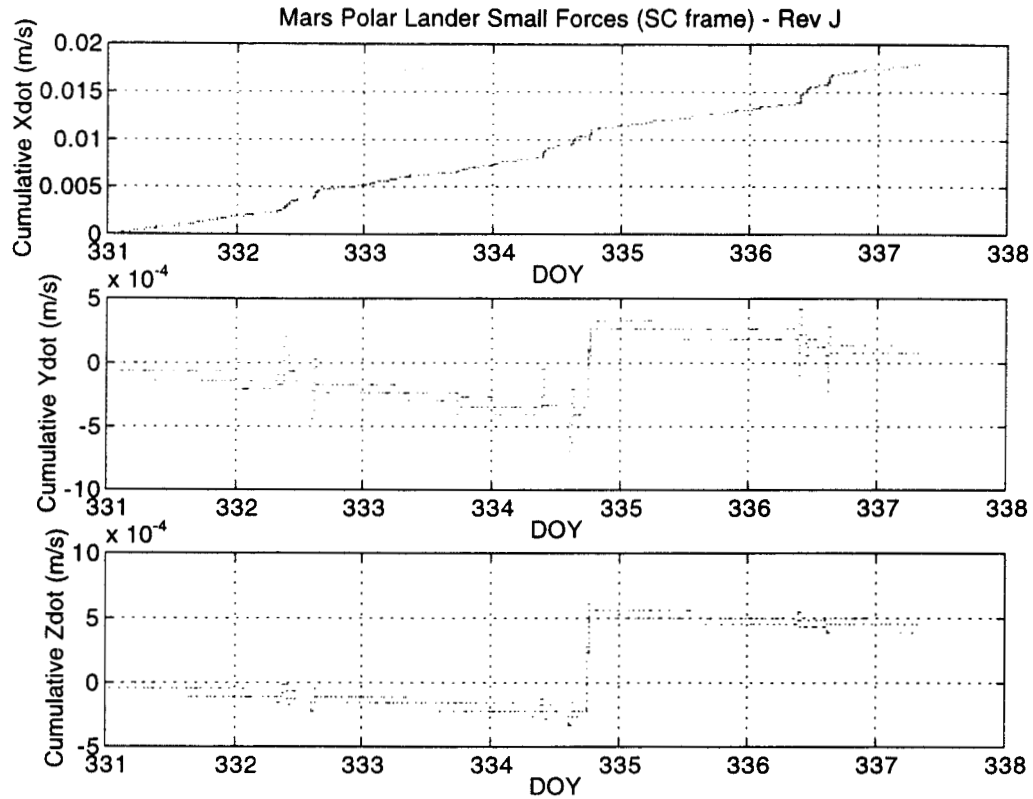


**Figure 6 Cumulative Velocity in the Spacecraft Frame**

The remaining portion of cruise did not include enough tracking data to finely calibrate the reported thruster activity. For example, communication was not normally maintained through the deadband walk periods. One test in late cruise involved the collection of two-way radiometric data during as much of a deadband walk and star camera processing period as possible, while recording high-rate telemetry data such as body rates. These data were analyzed and calibrations of the actual velocity imparted by the deadband walk were made to tune the reported velocity change in the small forces telemetry. Another area scrutinized was the actual thruster performance when single thruster pulses are far apart in time. This analysis, performed mainly by the NAG, was implemented in the attitude control velocity reconstruction used in the navigation analysis.

### **Solar Pressure Model**

The navigation software requires a spacecraft component model for computation of the acceleration imparted by solar radiation pressure. Specular and diffuse coefficients for each component are required as well to describe the amount of solar energy reflected and absorbed, along with the type of reflection. The spacecraft component model was defined in terms of the spacecraft coordinate frame definitions described earlier, so a single component model could be defined. The pre-launch spacecraft component model

used a flat plate to model the array and three flat plates oriented normal to the spacecraft coordinate frame axes to model the backshell. No components were included for the heat shield, since it was not illuminated by the Sun. This model assumed that the majority of cruise, especially late cruise, would have the solar array oriented directly at the Sun, with the X-Z plane in the Sun-probe-Earth plane. This orientation made the spacecraft symmetrical normal to the Sun line, allowing for the use of this model.

Once the attitude profile was changed in March, modification of the spacecraft component model was required due to the significant time spent with the solar arrays off-pointed from the Sun and due to the desire to improve the fidelity of the model. This new model, based on the Mars Pathfinder solar pressure model<sup>4</sup>, kept the flat plate for the solar array. Additional components were added to model the cruise ring, which was oriented the same way as the array but has a highly reflective gold covering, as opposed to the dark solar array. The original backshell model was replaced with a model that only includes the area that is not shaded by the solar array. Two components oriented along the backshell surface on each side of the array are used, with areas consistent with the component orientation used. The final solar pressure model used is detailed in Table 1.

## NAVIGATION STRATEGY

The main navigation requirement is to deliver the spacecraft to a safe landing in the designated target area. In terms of entry requirements, the flight path angle upon atmosphere entry (defined by a Mars-centered radial distance of 3522.2 km) is  $-13.25^\circ$  with a 95% probability that the flight path angle is within  $0.54^\circ$  of this value. The navigation strategy involves collecting radio metric tracking data at regular intervals for flight path estimation, predicting the arrival conditions, and performing occasional midcourse maneuvers, when needed, to correct the flight path such that the required arrival conditions are achieved.

After the formation of the NAG, a recommendation by this group was the collection of differenced Doppler and doubly-differenced range (DDR) measurements. The differenced Doppler data were processed by the navigation team but the DDR data was processed only by the NAG. The NAG also served as advisors for the formulation of the filter setup used for late cruise operations. The modeling improvements were discussed earlier, while the data collection and filter modeling are covered here.

**Table 1 Solar Pressure component model and orientation**

Component	Type	Dimensions	Spec	Diff	X <sub>sc</sub>	Y <sub>sc</sub>	Z <sub>sc</sub>
Solar Array	Flat Plate	4.14 m <sup>2</sup>	0.05	0.00	-1	0	0
Cruise Top	Flat Plate	0.70 m <sup>2</sup>	0.26	0.01	-1	0	0
Cruise Ring	Cylinder	H=0.4 m R=0.47 m	0.26	0.01	-1	0	0
Backshell	Flat Plate	0.43 m <sup>2</sup>	0.01	0.21	-0.707	0	0.707
Backshell	Flat Plate	0.43 m <sup>2</sup>	0.01	0.21	-0.707	0	-0.707

## Data Collection

The main tracking data types used during cruise were two-way Doppler and ranging data collected by the Deep Space Network (DSN). The maximum amount of tracking was limited by constraints on the solid state power amplifier (SSPA) maximum temperature and power available. These constraints translated into a maximum tracking duration of 4 hours, followed by a 5 hour off period. This tracking level was assumed for the first 30 days after launch and the last 45 days before Mars arrival. The tracking level during the remainder of cruise assumed one 4-hour tracking pass each day, with additional coverage before and after each trajectory correction maneuver (TCM).

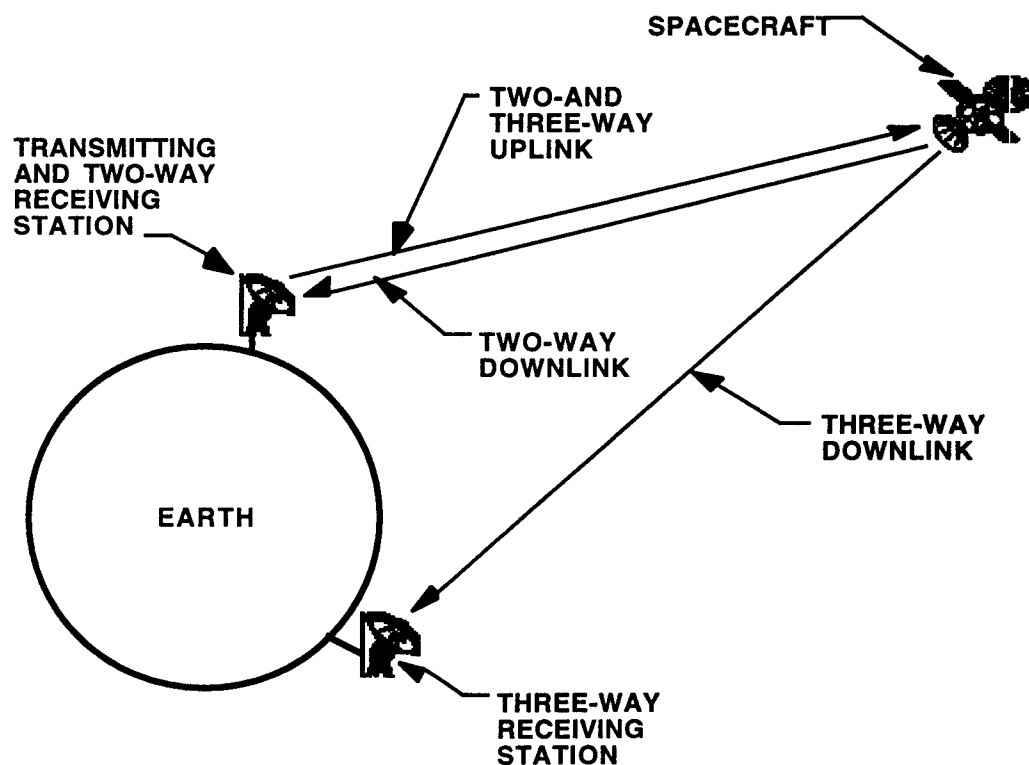
There were no specific concerns before launch concerning two-way Doppler data collection. However, two-way ranging acquisition was more problematic due to the more complex system required for accurate data collection. The biggest single data quality issue was two-way range data noise, which is strongly dependent on ranging signal power. As the power level drops, the range data noise increases. This problem was addressed both on the uplink (allocation of ground station power to the ranging signal) and the downlink (allocation of spacecraft transmitter power between ranging and telemetry functions). The uplink problem was addressed in two ways. All tracking passes during the last 45 days of cruise were required to originate from the 34m high efficiency (HEF) stations, with a 20kw transmitter, as opposed to the 34m beam wave guide (BWG) stations, with a 5kw transmitter. In addition, the transmitter power allocation to the range signal was increased. The downlink signal power was improved by allocating more spacecraft transmitter power to the ranging signal at the expense of telemetry data rate (most of this loss was recovered using a different telemetry encoding scheme). Additional range data noise improvements were achieved by adjusting the range system parameters, such as range signal code length.

After launch, data collection was nearly continuous while the star camera problems were worked. These tracking levels were reduced to the planned coverage after the first few weeks, with one pass per day maintained into October. Data were collected using both the HEF and BWG tracking stations through the first half of cruise, with most passes scheduled at the BWG stations. By July, the ranging data quality began to degrade. The degradation of the BWG range resulted in a change to longer range integration times in late July. At that time, the configuration setup did not allow different ranging configurations for the HEF and BWG stations, so all tracking stations were configured to generate range points every 30 minutes as opposed to the 5 minute integration time previously used. An update to the configuration files used by the stations, along with the spacecraft transmitter configuration change to allocate more power to the ranging signal, allowed for the collection of 10 minute HEF range data from early October to Mars encounter at or below the 1m noise requirement. The BWG range setup had 2.5m noise for the same time frame, but only a few BWG tracking passes were scheduled after mid-October.

Late in cruise, three-way Doppler data collection was added to the baseline two-way Doppler data collection. Three-way Doppler is available when a second tracking station receives the spacecraft signal originating from a different transmitting station, as shown in Figure 7. The difference of these simultaneous Doppler measurements was taken and processed as a separate data type. Differenced Doppler data, a measure of the velocity normal to the signal line of sight, was collected when there were overlaps in the view periods from two DSN complexes. This data requires accurate knowledge of the clock differences between the ground complexes to process effectively. These timing calibrations between the complexes were applied to the data processed for orbit determination. For MPL, the view periods for the Goldstone and Canberra complexes afforded the most overlapping coverage, so most of the data is along this baseline.

### **Near Simultaneous Tracking**

During the last 30 days of cruise, the tracking data collected from the lander was processed simultaneously with data collected from Mars Global Surveyor (MGS). By combining tracking data and estimating the trajectories of both spacecraft simultaneously, the effects of error sources that were common to both spacecraft were dramatically reduced, due to their high degree of correlation. The result of this technique, dubbed Near Simultaneous Tracking (NST), was a more accurate estimate of the lander's trajectory with respect to Mars than could have been obtained via reduction of the lander tracking data set only.



In order to reduce the chance of problems with the data collected for MPL approach, a demonstration phase was planned for MCO on its approach to Mars in September. This demonstration phase led to the identification and resolution of data collection problems that would have made the MPL NST data less accurate, such as the use of different signal paths for the two range sets. These modifications were in place when the MPL NST phase began in early November.

The approach adopted for the processing was to first fit data for MPL and MGS separately. The MGS solution included the state and other MGS-specific dynamic parameters, all the media parameters estimated for MPL, and the Mars ephemeris. The filter setup for MPL included the MPL state, dynamics and similar media and ephemeris parameters as for the MGS processing. Once separate converged solutions were generated, the resulting solutions were used as initial values for the combined filter. The MGS state was assumed fixed for this processing, while corrections were applied to the MPL solution when iteration was required.

### Orbit Determination Filter Setup

Orbit determination involves the determination of the flight path of the spacecraft using radio metric data and a discrete sequential filter for data reduction. In addition to the standard media (atmosphere, Earth platform) and dynamic (spacecraft state and solar pressure) parameters, the thruster-based attitude control system introduces dynamic uncertainty to the flight path which must be included in the filter. In addition to the media modeling, a data noise value is also used to account for data variations that are not otherwise modeled. The data noise modeling used is detailed in Table 2. Values for MGS are included here since the data was fit for the NST processing. Since both spacecraft were three-axis stabilized, no Doppler bias was required. The differenced Doppler data had applied timing calibrations but no additional bias was assumed or estimated. Ranging data had a pass-dependent bias assumed in the filter, both when processed for the single-spacecraft processing and when processed simultaneously. For the NST processing, an additional bias was estimated to account for frequency differences between the carrier that affects the path delay for each signal.

**Table 2 Data Types and Uncertainties**

Data Type	1 $\sigma$ uncertainty		Bias	
	MPL	MGS	MPL	MGS
Two-way Doppler	0.1 mm/s	0.25 mm/s	-	-
Two-way Range	1 m	1 m	1m, 5m	1 m
Two-way minus Three-way Doppler	0.05 mm/s	-	-	-
Near Simultaneous Tracking			25 cm	25 cm

The filter setup that was used for the late cruise OD analysis is detailed in Table 3. The philosophy used in developing the filter setup was based on Mars Pathfinder flight experience<sup>4</sup>. The main difference from traditional filter setup is the removal of consider parameters and instead including them in the estimate list, such as data errors due to atmosphere, Earth platform and station locations.

The dynamic modeling used for both solar pressure and the attitude control system had the most impact on the trajectory propagation. As such, a great deal of effort for both the modeling and the filter configuration was required. The solar pressure modeling, as described earlier, followed closely the Mars Pathfinder experience. The filter strategy also was based on Mars Pathfinder recommendations, which was to estimate area scaling factors for all the components and leave the physical properties of the components fixed. The area uncertainty used is a confidence level not only in the area inputs, but of the overall quality of the complete solar pressure model.

The plan for late cruise orbit determination was to have a baseline filter setup and a number of variations to that baseline to ensure that any required changes in the modeling assumptions could be determined quickly. The filter cases that were used at the end of cruise are described in Table 4. The variations were mostly in the data set, but variations in the small forces dynamic model were also included. In addition to the variations shown, additional variables included data arc length and small forces reconstruction modeling.

The main reason for the formalized filter configurations was to make the time from data reception through the generation of filter solutions that adequately cover the space of possible solutions as short as possible. With this setup, the likelihood of requiring changes to the filter setup in a time-critical situation was small. This was the case for TCM5, which required a maneuver execution of E-6.5 hours with data up to E-12 hours, with a backup data cutoff of E-14 hours. The purpose of TCM5 was to have the opportunity to execute a maneuver to change the flight path angle if the likely entry point was outside a specified limit. To allow the data cutoff at E-12 hours, a suite of 10 maneuvers was designed to change the flight path angle while keeping the other entry parameters constant. The set of maneuvers had only two pointing vectors, with five maneuvers to increase the flight path angle by  $0.25^\circ$  increments and five to decrease the flight path angle in the same fashion. Provision was included in the TCM5 decision process to execute a TCM5 maneuver if the expected landing site presented a hazard.

The criteria used for the TCM5 decision was to execute the maneuver if the best solution was outside  $\pm 0.3^\circ$  of the target flight path angle of  $-13.25^\circ$  (recall that the spacecraft survivability limits were  $\pm 1.0^\circ$  or about 20 km in B•T). If this were true, the direction (increase or decrease) and the magnitude that best matches the desired change were selected and transmitted to the spacecraft. If the solution were within  $\pm 0.3^\circ$ , then no TCM5 would be executed.

**Table 3 Filter Setup for late cruise OD analysis**

<b>Filter Parameter</b>	<b><i>a priori</i> uncertainty (1<math>\sigma</math>)</b>	<b>Process Noise (N/A for bias parameters)</b>	<b>Correlation time (N/A for bias parameters)</b>	<b>Comments</b>
Initial position and velocity	1000 km and 10 m/s	N/A	N/A	
Solar Pressure	5% of component area	N/A	N/A	Estimate area only
Constant Acceleration (X, Y, Z) <sub>sc</sub>	1.00E-11 km/s <sup>2</sup> , 5.00E-12 km/s <sup>2</sup> , 5.00E-12 km/s <sup>2</sup>	N/A	N/A	1.5E-11 km/s <sup>2</sup> nominal X
Lander attitude control activity	10% or 30% of total	10% or 30% of total	0 hours	Stochastic, 1 hour updates
Maneuver Crosstrack	0.66%, $\Delta V < 0.5$ m/s 3.3%, $\Delta V > 0.5$ m/s	N/A	N/A	Function of maneuver magnitude
Maneuver Magnitude	0.01 m/s + 0.66%	N/A	N/A	Function of maneuver magnitude
Maneuver slews	10% of RSS slew magnitude, 400s on impulse time	N/A	N/A	Estimate impulse + time offset
Safe Mode Slews	30% of RSS slew magnitude, 1200s on impulse time	N/A	N/A	Estimate impulse + time offset
Station Range Bias	1 m (7RU)	1 m (10 RU) or 5 m (35 RU)	0 hours	Pass-dependent bias
Troposphere	4 cm (wet) 1 cm (dry)	4 cm (wet) 1 cm (dry)	6 hours (wet) 2 hours (dry)	Stochastic, 1 hour updates
Ionosphere	3 cm (day) 1 cm (night)	3 cm (day) 1 cm (night)	5 hours (day) 24 hours (night)	Stochastic, 1 hour updates
Station locations	Full covariance	N/A	N/A	
Polar motion	5 cm	5 cm	48 hours	Stochastic, 4 hour updates
Earth rotation	0.3 ms	0.3 ms	24 hours	Stochastic, 4 hour updates
Mars ephemeris	Full covariance	N/A	N/A	

**Table 4 Filter Case Description**

Case #	Data Used				Constant Acceleration	Stochastic Acceleration	Range Bias
	Doppler	Range	Differenced Doppler	NST			
1	√	√	√	√	√	10%	1 m
2	√	√	√	√	√	10%	5 m
3	√	√	√	√	√	30%	1 m
4	√	√	√		√	10%	1 m
5	√	√		√	√	10%	1 m
6	√	√	√	√		10%	1 m

## RESULTS

The results presented are all for solutions generated after the execution of TCM4, which was at E-3 days or November 30. These results for the B-plane components are presented in Figures 8 and 9 as a function of time for a number of solutions. The same data is shown in the B-plane in Figure 10. The  $\pm 0.3^\circ$  corridor for TCM5 execution is shown as well in Figure 8. The solutions shortly after TCM4 have nearly a 15km variation in the B•R direction, which maps almost directly into flight path angle. Note that the flight path angle variation before TCM4 was around 6 km. The early solutions after TCM4 were all at or below the target flight path angle. This trend continued with solutions using data up to E-36 hours. The B•T values started at or East of the target, with the solutions at E-36 hours maintaining the Eastward trend. At this point, a decision was made to replace the original five maneuvers to decrease the flight path angle with a set of maneuvers that both increased the flight path angle and moved the B•T value closer to the target. These maneuvers were tested and ready to go when the next set of solutions was obtained.

At E-20 hours, the solutions shifted significantly in the B•R direction, such that several cases now fell above the flight path angle target. At this point the replacement maneuvers were abandoned and the original set of maneuvers to decrease the flight path angle were maintained. The B•T offset continued to increase as the solution moved along the major axis of the error ellipse, but it was too late at this point to design maneuvers that would both decrease the flight path angle and move B•T.

At E-12 hours the flight path angle results were all below the target, with the spread of solutions centered at the  $+0.3^\circ$  point, or the limit for the no-execute decision. It was decided that the best course of action was to execute a TCM5 to decrease the flight path angle by the minimum designed value. The main arguments against executing TCM5



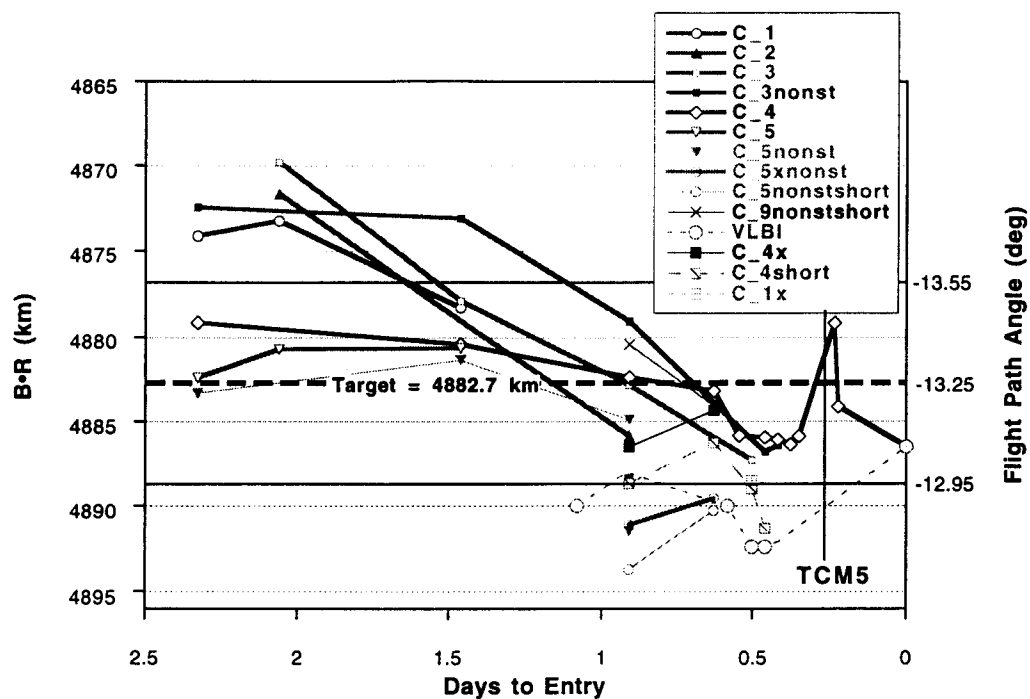


Figure 8 B•R History as a function of Data Cutoff

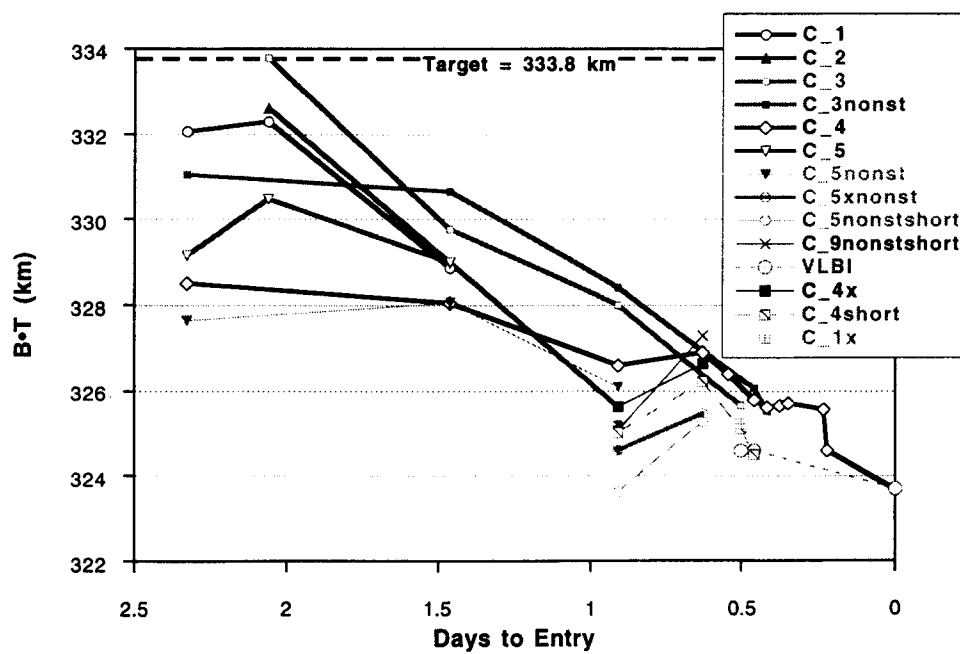
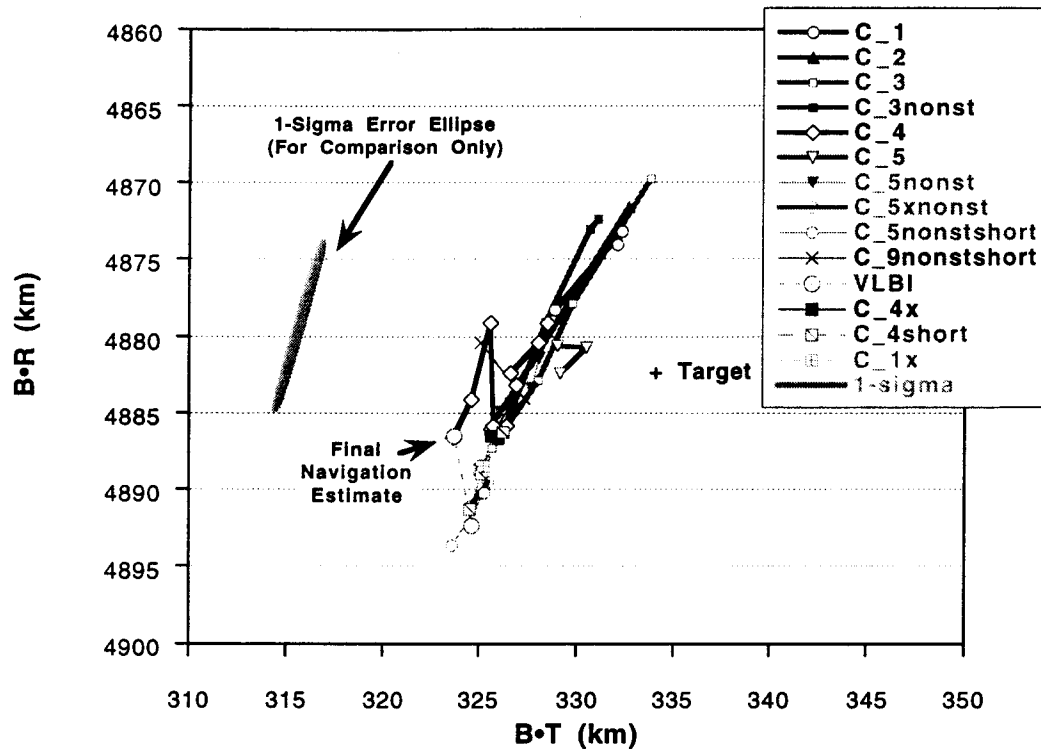


Figure 9 B•T History as a function of Data Cutoff



**Figure 10 B-plane variation relative to Data Cutoff**

were that the spacecraft was well within the  $\pm 1.0^\circ$  corridor and on the edge of the no execute zone.

After execution of TCM5, a solution was generated but had only a few minutes of post-maneuver data. The spacecraft re-oriented after the maneuver for a four-hour star camera update period for the final inertial measurement unit (IMU) update before entry, which meant that no tracking data would be collected until nearly 4.5 hours after the maneuver execution. Once data collection resumed at E-1 hour, the spacecraft was deep enough in the Mars gravity well that a data arc starting post-TCM5 could be processed to generate solutions. These solutions, which were relayed to the team during the last hour of approach, could be generated quickly using data collected in real time. The final entry state, using tracking data up to the turn to entry attitude and loss of contact with the DSN, is shown at E-0.

The coupling of the  $B \cdot R$  and  $B \cdot T$  drift is best illustrated with the B-plane plot in Figure 10. The data shown are the same as the data presented previously, with a 1-sigma error ellipse shown for comparison. The variations in the solution are along the major axis of

the error ellipse, as expected, except for changes due to execution of TCM4 and TCM5. The reasons for the change in B•T are still being investigated, but the shift is partially due to maneuver execution errors.

## **ACKNOWLEDGEMENTS**

The authors would like to thank the Navigation Advisory Group, chaired by Joseph Guinn and Michael Watkins, for their support. The list of people who lent assistance to the navigation team through the NAG either through analysis or lending expertise is quite long, and their efforts and weird hours are appreciated.

The work described in this paper was performed at the Jet Propulsion Laboratory, California Institute of Technology, under contract with the National Aeronautics and Space Administration.

## **REFERENCES**

1. McNamee, J. B., "The 1998 Mars Surveyor Lander and Orbiter Project." 35th Space Congress, Cocoa Beach, Florida, April 28 - May 1, 1998.
2. Mars Surveyor '98 Project Policies and Requirements Document (JPL internal document).
3. Kallemeyn, P. H., P. C. Knocke, P. D. Burkhart and S. W. Thurman, "Navigation and Guidance for the Mars Surveyor '98 Mission", AIAA Astrodynamics Specialist Conference, Boston, MA August 10-12 1998.
4. Mars Pathfinder Navigation Report (JPL internal document).